Ramirez Hoyos, P.; Cervera Montesinos, J.; Ali, M.; Nasir, S.; Ensinger, W.; Mafe, S. (2020). Impact of Surface Charge Directionality on Membrane Potential in Multi-ionic Systems. The Journal of Physical Chemistry Letters. 11(7):2530-2534. https://doi.org/10.1021/acs.jpclett.0c00554

Impact of surface charge directionality and pore shape on the membrane potential of multi-ionic systems

Patricio Ramirez[†,*] Javier Cervera[‡] Mubarak Ali,[§,‖] Saima Nasir, [§,‖] Wolfgang Ensinger,[‖] and Salvador Mafe[‡,*]

[†]Departamento de Física Aplicada, Universitat Politécnica de València, E-46022 València (Spain)

[‡]Departament de Física de la Terra i Termodinàmica, Universitat de València, E-46100 Burjassot (Spain)

[§]Materials Research Department, GSI Helmholtzzentrum für Schwerionenforschung, D-64291 Darmstadt (Germany)

[‖]Department of Material- and Geo-Sciences, Technische Universität Darmstadt, D-64287 Darmstadt (Germany)

Supporting Information

ABSTRACT: The membrane potential (V_{mem}) defined as the electric potential difference across a membrane flanked by two different salt solutions is central to electrochemical energy harvesting and conversion. Also, V_{mem} and the ionic concentrations that establish it are important to biophysical chemistry because they regulate crucial cell processes. We study experimentally and theoretically the salt dependence of V_{mem} in single conical nanopores for the case of multi-ionic systems of different ionic charge numbers. The major advances of this letter are: (*i*) to measure V_{mem} using a series of ions (Na^+, K^+, Ca^{2+}, Cl^-, and SO_4^{2-}) that are of interest to both energy conversion and cell biochemistry, (*ii*) to describe the physicochemical effects resulting from the nanostructure asymmetry, (*iii*) to develop a theoretical model for multi-ionic systems, and (*iv*) to quantify the role of the liquid junction potentials established in the salt bridges to the total cell membrane potential.

The membrane potential (V_{mem}) is the difference of electric potential across a membrane flanked by two different aqueous salt solutions. Experimentally, V_{mem} can be measured as the external voltage that should be applied to maintain a null current through the membrane, the so-called *reversal potential*.[1,2] This physicochemical magnitude quantifies the conversion between the chemical energy available as a salt concentration gradient and the electrical energy that can be obtained from the resulting potential difference.[3-5] Moreover, V_{mem} and the ionic concentrations that establish it are also important in biophysical chemistry because this potential difference regulates crucial cell processes.[1,6,7]The asymmetric nanopores that are employed in electrochemical energy conversion[4,5] constitute artificial nanostructures that mimic the ion channel proteins of cell membranes when biologically relevant ions (e.g., potassium, calcium, and chloride) are involved[1,7,8]

We explore here, experimentally and theoretically, the salt dependence of V_{mem} in single conical nanopores for the case of multi-ionic systems and concentrations relevant to membrane bioelectrochemistry. These nanoscale pores are functionalized with an asymmetric axial distribution of carboxylic acid groups on the pore surface, which is also the case of protein ion channels.[1,9] Both nanopores and ion channels show ionic selectivity because of the interaction between the mobile ions in solution and the charges fixed on the pore surface.

The major advances of this work are: (*i*) to measure V_{mem} using ions (Na^+, K^+, Ca^{2+}, Cl^-, and SO_4^{2-}) that are of interest to both energy conversion and cell biochemistry, (*ii*) to describe the physicochemical effects resulting from the nanostructure asymmetry, (*iii*) to develop a complete theoretical model for multi-ionic systems, and (*iv*) to quantify the contribution of the liquid junction potentials established in the salt bridges to the total cell membrane potential. Because of the marked interdisciplinary nature of the problem, these results should be of immediate significance to a broad physical chemistry audience.

Figure 1 shows the scheme of the experimental system.[10] All measurements are conducted for two nanopore (NP) orientations and a couple of Ag|AgCl electrodes with 2M KCl salt bridges immersed in the left (L) and right (R) bathing solutions. Figure 2 shows the experimental set-up (*left*) and procedure (*right*) used to measure the membrane potential as the reversal potential $V_{mem} = V(I = 0)$, where $V = V_L - V_R$ is the applied potential difference (voltage) and I is the current.

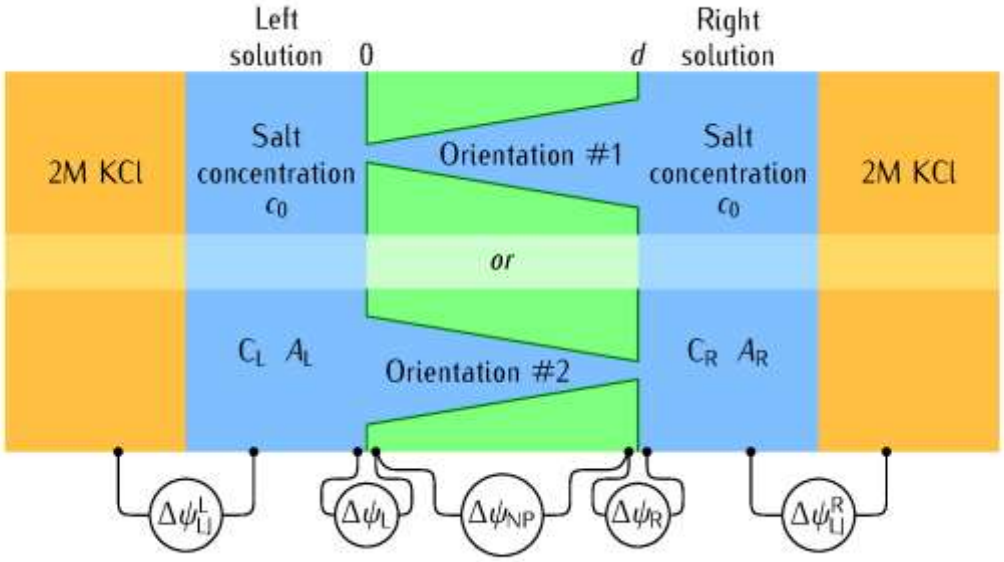

Figure 1. Scheme of the experimental system. The single-pore membrane is flanked by two *different* salt solutions at the *same* concentration c_0 whose *pH* is kept close to neutral values. The cations considered are $C_L = Na^+$, Ca^{2+}, or K^+, with $C_R = K^+$, while the anions considered are A_L and $A_R = Cl^-$ or SO_4^{2-}. In our case, we take V_{mem} as the *total electric potential drop* (the cell membrane potential), which depends on the particular pore orientation. Note that V_{mem} is then composed by the liquid junction potentials established in the salt bridges ($\Delta\psi_{LJ}^{L}$ and $\Delta\psi_{LJ}^{R}$), the Donnan potentials at the two membrane-solution interfaces ($\Delta\psi_L$ and $\Delta\psi_R$), and the diffusion potential in the nanopore ($\Delta\psi_{NP}$).[10,11] The liquid junction potentials can be calculated by means of the Henderson equation by assuming ideal solutions that mix continuously following identical functional dependences for all ionic concentrations.[2,12] The equations allowing estimations of these potentials can be found in the *Supporting Information*.

The curves shown in Figure 2 (*right*) correspond to the smallest concentrations used in the experiments (2 mM). At this concentration, the measured currents are in the range of 10 pA and show the highest scatter in the experimental data, leading to uncertainties around 5% in the reversal potential obtained from each individual *I*–*V* curve. Each experimental point corresponds to at least three independent measurements using the same sample and electrolyte concentrations. This procedure gives an upper limit (low concentrations limit) in the range 10–15 % for the uncertainty in the reversal potentials.

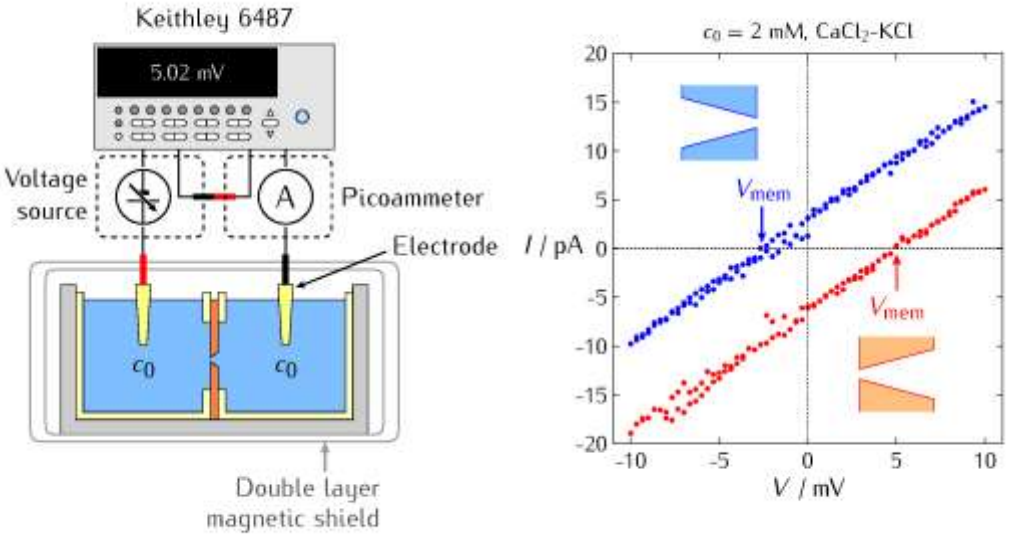

Figure 2. Scheme of the experimental set-up (*left*) and the measurement of V_{mem} as the reversal potential $V_{mem} = V(I = 0)$ (*right*). The electrochemical cell is placed within a double layer magnetic shield placed on an anti-vibration table to avoid external perturbations. Note that the two cases shown correspond to the smallest concentrations used in the experiments, which lead to the highest scatter and experimental uncertainties in the currents measured.

Figures 3 (experimental data) and 4 (model results) show the V_{mem} *vs.* c_0 curves. The theoretical curves of Figure 4 are calculated using the constant field solution of the Nernst-Planck flux equations for a system of three ions whose cations or anions have different charge numbers (Figure 1). The pore fixed-charge asymmetry can then be incorporated in the cubic or

quadratic equations obtained for the interfacial concentrations (*Supporting Information*). This approximated procedure gives relatively simple *analytical* solutions that provide useful qualitative insights, as opposed to more exact but *numerical* solutions of the Poisson-Nernst-Planck model for multi-ionic systems. In particular, our approach leads to explicit equations that give a clear physical understanding of the different potential drops of Figure 1, allowing a direct estimation of the liquid junction potentials (Figure 4). The *Supporting Information* gives detailed derivations of all relevant equations for the four cases of Figure 4.

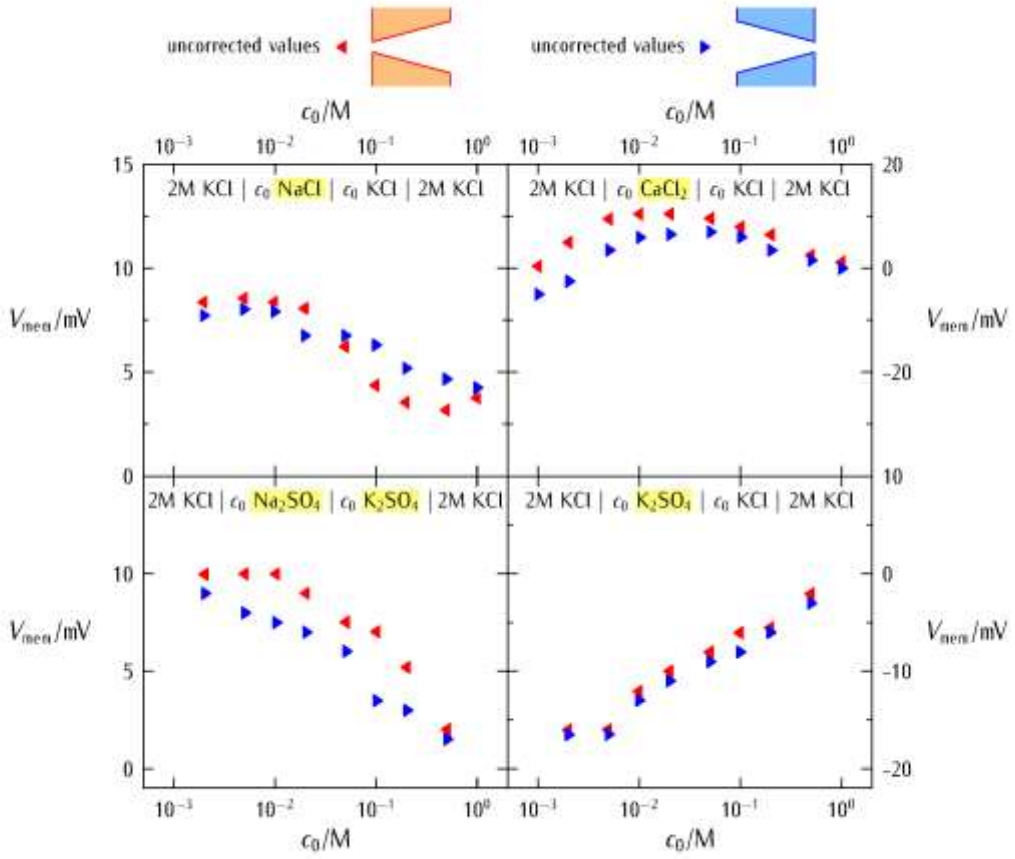

Figure 3. Experimental V_{mem} *vs.* c_0 curves for the different multi-ionic systems considered (*insets*) and the two pore orientations of Figure 1. The data correspond to the measured cell membrane potentials and are not corrected by the liquid junction potentials of Figure 1. Salts other than KCl are highlighted for the sake of clarity. Note the different scales of V_{mem} obtained in each case.

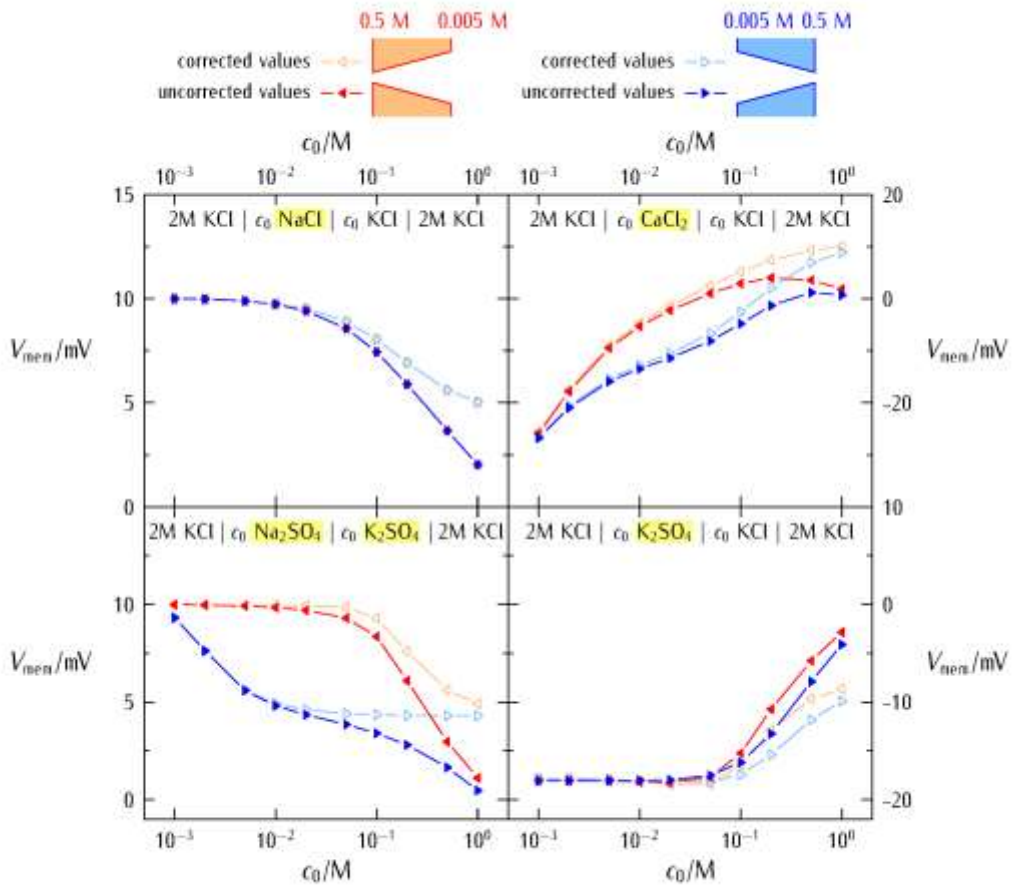

Figure 4. Theoretical V_{mem} *vs.* c_0 curves for the different multi-ionic systems considered (*insets*) and the two pore orientations. Henderson equation-corrected and uncorrected V_{mem} values are shown to emphasize the relevant role of the two liquid junction potentials of Figure 1. The pore volume charge concentrations $X(0)$ and $X(d)$ assumed in the model constitute typical pore tip and base values, respectively.[2] For instance, by introducing a surface charge density σ = 0.9 e/nm^2, the volume charge concentrations $X(0) = 2\sigma/(Fa_{tip})$ = 0.5 M (pore tip radius a_{tip} = 6 nm) and $X(d) = 2\sigma/(Fa_{base})$ = 0.005 M (pore base radius a_{base} = 600 nm) are obtained (orientation # 1), where e is the elementary charge and F is the Faraday constant.

The experimental membrane potentials of Figure 3 show significant differences for the two orientations of the asymmetric nanopore, except for the case corresponding to the *same* cation (K^+) at solutions L and R. This fact clearly shows that the negative pore surface charges select cations to anions. In general, the pore directionality effect results from the different

screening of the pore tip charges by the distinct cations as well as the charge number-dependent ionic exclusion of the anions. Asymmetric effects are also significant in protein ion channels.[1,9,13] Note also that the absolute values of V_{mem} tend to decrease in the limit of high salt concentration because of the high Debye screening of the pore charges.[2]

For the particular case of the NaCl–KCl system, the interfacial Donnan potentials of Figure 1 cancel out and V_{mem} is simply the diffusion potential in the nanopore, which is non-zero because of the different cations in the solutions. For the case of a symmetrical membrane at *low* salt concentration, $V_{bip} = (RT/F)\ln(D_{+R}/D_{+L})$, which depends only on the diffusion coefficients D_{+L} and D_{+R} of the two cations in the left and right solutions, since the co-ion (Cl^-) is excluded from the pore.[2,14] Here, T is the temperature and R the gas constant. By introducing the ionic diffusion coefficients at infinite dilute solution, V_{bip} = 10 mV which is close to the experimental result of Figure 3. On the contrary, the pore solution mobile ions can screen the nanopore charges at *high* salt concentration. Thus, the chloride ion is not excluded and contributes to V_{mem} with a diffusion coefficient D_-. By using the Goldman equation[2,14] $V_{mem} = (RT/F)\ln[(D_{+R}+D_-)/(D_{+L}+D_-)]$ = 4 mV for the effective liquid junction potential established between the two monovalent salts, also in agreement with the experimental result of Figure 3.

For the $CaCl_2$–KCl system, V_{mem} can take high and positive values because of the different cation diffusion coefficients and the chloride concentration gradient favoring $V_{mem} > 0$ (Figure 1). Remarkably, a maximum is found at intermediate concentrations because of the interplay between the Donnan potentials dominant at low ionic concentration and the nanopore diffusion potential dominant at high concentration (Figure 1). As to the Na_2SO_4–K_2SO_4 system, the V_{mem} values are similar to those of the NaCl–KCl system because of the anion (SO_4^- or Cl^-) exclusion from the pore. For the K_2SO_4–KCl case, however, it is the potassium concentration gradient that gives $V_{mem} < 0$ at low concentrations where the ions SO_4^- or Cl^- are excluded from

the pore solution because of the significant electrostatic repulsion by the unscreened negative pore charges.

For the sake of comparison, we use the same scales for the V_{mem} values in Figure 4 and in Figure 3. However, no attempt was made to fit the theoretical curves to the experimental data because of the qualitative nature of the model, which can describe only the experimental trends. We believe that the model equations of the *Supporting Information* are useful because: (*i*) they approximately reproduce the experimental range of observed V_{mem} values in most cases, (*ii*) they provide explanations concerning the differences obtained for the two orientations of the asymmetric nanopore in terms of the potential drops of Figure 1, and (*iii*) they show that the contribution of the liquid junction potentials to V_{mem} cannot be neglected in the high salt concentration limit, allowing also a convenient estimation of these potentials in each experimental case (Figure 4). Recently, the reversal potential of monolayer graphene and hexagonal boron nitride membranes[15] and the open-circuit voltage of proton selective composite membranes[16] have also been analyzed by using the Goldman potential equation. Also, the segmentation potential model of Figure 1, together with the experimental method of Figure 2, could be useful in other electrochemical contexts concerning solid/liquid interfaces.

In conclusion, we have shown that many physico-chemical phenomena including the nanostructure directionality and surface charge, the ionic charge numbers and concentrations, and the different potential drops of Figure 1 contribute to the measured cell membrane potentials. Also, we have obtained explicit analytical equations that give a useful qualitative description of the basic physical chemistry involved.

■ ACKNOWLEDGMENTS

M. A., S. N., and W. E. gratefully acknowledge the financial support from the Hessen State Ministry of Higher Education, Research and the Arts (Germany), LOEWE project iNAPO. P.

R., J. C., and S. M. acknowledge the funding from the *Ministerio de Economia y Competitividad* and the European Regional Development Funds (FEDER), project MAT2015-65011-P.

■ MATERIALS AND METHODS

The nanopore fabrication and characteristics have been described with detail previously.[2] The base and tip radii can obtained by imaging the pore and measuring the electrical conductane.[17-19] These radii are typically in the range a_{base} = 300 – 800 nm and a_{tip} = 10 – 40 nm.[20] The pore surface charge density is in the range σ = 0.2 – 1 e/nm^2, as obtained from the I–V curves measured at neutral pH.[17,20-22] The effect of pore charge inversion was studied previously for the cases of the I–V curves[23] and the reversal potential,[24] and was found significant for trivalent (La^{3+}) cations, which is not the case considered here. The reliability of the experimental approach and the data statistics were checked previously with both an Axopatch 200B and the picoammeter of Figure 2.[2] The experimental determination of V_{mem} requires to control currents of the order of 10 pA with the picoammeter (Keithley Instruments, Cleveland, Ohio) and avoid external perturbations by placing the measuring electrochemical cell within a double layer magnetic shield (Amuneal Manufacturing, Philadelphia, PA) placed on an anti-vibration table (Gimbal Piston, Ametek Tech., Berwyn, PA).. We have mentioned this fact in pg. 10 of the revised manuscript.

■ ASSOCIATED CONTENT

Supporting Information

The *Supporting Information* is available free of charge at https://pubs.acs.org/doi/ and gives a detailed description of the theoretical model and the different salt systems studied (PDF).

■ AUTHOR INFORMATION

Corresponding Authors

*E-mail: patraho@fis.upv.es (P.R.).

*E-mail: smafe@uv.es (SM.).

ORCID

P. Ramirez: https://orcid.org/0000-0002-0067-4887

J. Cervera: https://orcid.org/0000-0001-8965-9298

M. Ali: https://orcid.org/0000-0002-2521-2718

S. Mafe: https://orcid.org/0000-0003-3248-7020

Author Contributions

All authors contributed significantly to the manuscript.

Notes

The authors declare no competing financial interest.

■ REFERENCES

(1) Hille, B. *Ion channels of excitable membranes*, 2nd ed; Sinauer Associates: Sunderland, **1992**.
(2) Ramirez, P.; Cervera, J.; Gomez, V.; Ali, M.; Nasir, S.; Ensinger, W.; Mafe, S. Membrane potential of single asymmetric nanopores: Divalent cations and salt mixtures. *J. Membrane Sci.* **2019**, *573*, 579–587.
(3) Sales, B.; Saakes, M.; Post, J. W.; Buisman, C. J. N.; Biesheuvel, P. M.; Hamelers, H. V. M. Direct power production from a water salinity difference in a membrane-modified supercapacitor flow cell. *Environ. Sci. Technol.* **2010**, *44*, 5661–5665.
(4) Li, R.; Jiang, J.; Liu, Q.; Xie, Z.; Zhai, J. Hybrid nanochannel membrane based on polymer/MOF for high performance salinity gradient power generation. *Nano Energy* **2018**, *53*, 643–649.
(5) Balme, S.; Ma, T.; Balanzat, E.; Janot, J. M. Large osmotic energy harvesting from functionalized conical nanopore suitable for membrane applications. *J. Power Sources* **2017**, *544*, 18–24.
(6) Cervera, J.; Pietak, A.; Levin, M.; Mafe, S. Bioelectrical coupling in multicellular domains regulated by gap junctions: a conceptual approach. *Bioelectrochem.* **2018**, *123*, 45–61.
(7) Yang, M.; Brackenbury, W. J. Membrane potential and cancer progression. *Front. Physiol.* **2013**, *4*, 185.
(8) Lepoitevin, M.; Ma, T.; Bechelany, M.; Janot, J. M.; Balme, S. Functionalization of single solid state nanopores to mimic biological ion channels: A review. *Adv. Colloid Interface Sci.* **2017**, *250*, 195–213.
(9) Queralt-Martín, M.; Garcia-Gimenez, E.; Aguilella, V. M.; Ramírez, P.; Mafé, S.; Alcaraz, A. Electrical pumping of potassium ions against an external concentration gradient in a biological ion channel. *Appl. Phys. Lett.* **2013**, *103*, 043707.
(10) Kontturi, K.; Murtomäki, L.; Manzanares, J. A. *Ionic transport processes: in Electrochemistry and Membrane Science*, Oxford University Press: New York, **2008**.
(11) Galama, A. H.; Post, J. W.; Hamelers, H. V. M.; Nikonenko, V. V.; Biesheuvel, P. M. On the origin of the membrane potential arising across densely charged ion exchange membranes: How well does the Teorell-Meyer-Sievers theory work? *J. Membrane Sci. Res.* **2016**, *2*, 128–140.
(12) Garcia-Gimenez, E.; Alcaraz, A.; Aguilella, V. M ; Ramirez, P. Directional ion selectivity in a biological nanopore with bipolar structure. *J. Membrane Sci.* **2009**, *331*, 137–142.

(13) Verdia-Baguena, C.; Gomez, V.; Cervera, J.; Ramirez, P.; Mafe, S. Energy transduction and signal averaging of fluctuating electric fields by a single protein ion channel. *Phys. Chem. Chem. Phys.* **2017**, *19*, 292–296.
(14) Guirao, A.; Mafé, S.; Manzanares, J. A.; Ibáñez, J. A. Biionic potential of charged membranes: Effects of the diffusion boundary layers. *J. Phys. Chem.* **1995**, *99*, 3387–3393.
(15) Caglar, M.; Silkina, I.; Brown, B. T.; Thorneywork, A. L.; Burton, O. J.; Babenko, V.; Gilbert, S. M.; Zett, A.; Hofmann, S.; Keyser, U. F. Tunable Anion-Selective Transport through Monolayer Graphene and Hexagonal Boron Nitride. *ACS Nano* **2020**, doi: 10.1021/acsnano.9b08168.
(16) Shinde, D. B.; Vlassiouk, I. V.; Talipov, M. R.; Smirnov, S. N. Exclusively Proton Conductive Membranes Based on Reduced Graphene Oxide Polymer Composites. *ACS Nano* **2019**, *13*, 13136–13143.
(17) Siwy, Z.; Fulinski, A. Fabrication of a Synthetic Nanopore Ion Pump. *Phys. Rev. Lett.* **2002**, *89*, 198103.
(18) Siwy, Z.; Dobrev, D.; Neumann, R.; Trautmann, C.; Voss, K. Electro-responsive asymmetric nanopores in polyimide with stable ion-current signal. *Appl. Phys. A* **2003**, *76*, 781–785.
(19) Apel, P. Track etching technique in membrane technology. *Radiat. Meas.* **2001**, *34*, 559–566.
(20) Ramirez, P.; Garcia-Morales, V.; Gomez, V.; Ali, M.; Nasir, S.; Ensinger, W.; Mafe, S. Hybrid circuits with nanofluidic diodes and load capacitors. *Phys. Rev. Applied* **2017**, *7* 064035.
(21) Ramirez, P.; Apel, P. Y.; Cervera, J.; Mafe, S. Pore structure and function of synthetic nanopores with fixed charges: Tip shape and rectification properties. *Nanotechnology* **2008**, *19*, 315707.
(22) Vlassiouk, I.; Smirnov S.; Siwy Z. Nanofluidic ionic diodes. Comparison of analytical and numerical solutions. *ACS Nano* **2008**, *2*, 1589–1602.
(23) Ramirez, P.; Manzanares, J. A.; Cervera, J.; Gomez, V.; Ali, M.; Pause, I.; Ensinger, W.; Mafe, S. Nanopore charge inversion and current-voltage curves in mixtures of asymmetric electrolytes. *J. Membrane Sci.* **2018**, *563*, 633–642
(24) Nasir, S; Ali, M.; Cervera, J.; Gomez, V.; Haider, M. H. A.; Ensinger, W.; Mafe, S.; Ramirez, P. Ionic transport characteristics of negatively and positively charged conical nanopores in 1:1, 2:1, 3:1, 2:2, 1:2, and 1:3 electrolytes. *J. Colloid Interface Sci.* **2019**, *553*, 639–646.

TOC image

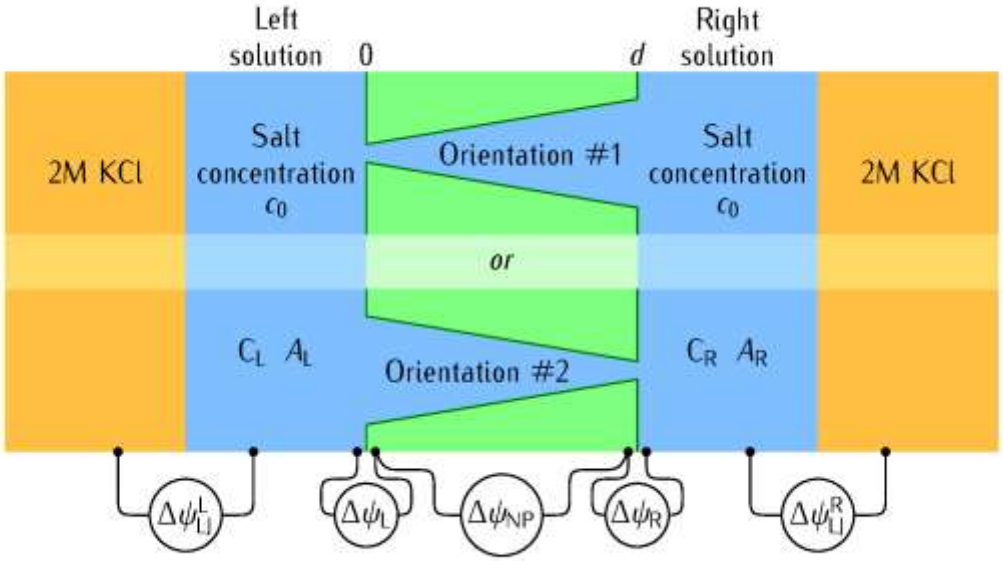

Keywords

Physical chemistry of nanopores, biomimetic membranes, asymmetrical nanostructures, theoretical modeling, divalent cation